Environmental Science and Pollution Research (2023) 30:109751–109768
https://doi.org/10.1007/s11356-023-29848-0

RESEARCH ARTICLE

Efficient Cr(VI) sequestration from aqueous solution by chemically modified *Garcinia kola* hull particles: characterization, isotherm, kinetic, and thermodynamic studies

Lekan Taofeek Popoola[1]

Received: 7 December 2022 / Accepted: 8 September 2023 / Published online: 30 September 2023

Abstract

There is a need for the removal of hexavalent chromium from contaminated water prior to its discharge into the environment, as part of industrial effluents, due to its toxic nature. In this present study, an adsorbent prepared via chemical modification of *Garcinia kola* hull particles (GK-HP) using NaOH was applied for Cr(VI) sequestration from aqueous solution. Both the raw (rGK-HP) and chemically modified *Garcinia kola* hull particles (cMGK-HP) were characterized using BET, SEM, XRD, FTIR, TGA, and EDS. The effects of pH, contact time, adsorbent dose, adsorbate initial concentration, and temperature on Cr(VI) sequestration were examined. The adsorbent, cMGK-HP, proved to be more effective for the adsorption process than rGK-HP with 96.25% removal efficiency at a pH of 2, a contact time of 60 min, an adsorbent dose of 5 g/L, Cr(VI) initial concentration of 20 mg/L and a temperature of 40°C. Isotherm and kinetic studies showed experimental data to be well-fitted with Langmuir isotherm and follow the pseudo-second-order kinetic model. The thermodynamic study revealed adsorption nature to be feasible, occur via physisorption, spontaneous, and exothermic. Changes in morphological structure, textural property, spectral peak, phase composition, and chemical composition of adsorbents before and after Cr(VI) sequestration from solution were proved by SEM, BET, FTIR, XRD, and EDS analyses, respectively. cMGK-HP possessed excellent reusability attribute and high thermal stability as shown by TGA. In conclusion, the adsorption capacity of cMGK-HP is better than many other adsorbents generated from agrowastes used in previous studies for Cr(VI) removal.

Keywords *Garcinia kola* · Chemical modification · Chromium · Kinetic · Thermodynamic

Introduction

Chromium exists in two forms as either trivalent or hexavalent (Ogata et al. 2018), but the latter is more carcinogenic and mutagenic to human beings and animals (Fernandez et al. 2018) with toxicity of about 500 times more than the former (Qiu et al. 2018). Cr(VI) poses a threat to the ecological environment (Yulizar et al. 2016) and human respiratory tract, kidney, liver, immune, and gastrointestinal systems when absorbed into the body system at low concentration (Yao et al. 2020). Its maximum permissible discharge limit stated by the World Health Organization (WHO) is 0.05 mg/L (Li et al. 2019). However, rapid industrialization and agricultural activities have made the use of Cr(VI) to be unavoidable. Hexavalent chromium is used for different applications in various manufacturing and industrial companies engaged in steel fabrication, electroplating, wood preservatives, paints and pigments, metal finishing, canning, tanneries, and many more (Song et al. 2021). Thus, industrial wastewater containing chromium from these industries are irrationally discharged into the environment causing soil and water pollution (Fernandez et al. 2018). Nonetheless, chromium is one of the constituents of pesticides which are widely used for agricultural purposes (Hamilton et al. 2018). Chromium wastewater finds its way through surface runoff into rivers and lakes or via permeation into groundwater (Ali and Saeed 2015). Therefore, it is imperative to treat Cr(VI)-wastewater before discharging to keep our environment safe.

So far, adsorption has been tagged as an effective way of remediating and removing Cr(VI) from wastewater among

Responsible Editor: Ioannis A. Katsoyiannis

✉ Lekan Taofeek Popoola
ltpopoola@abuad.edu.ng; popoolalekantaofeek@yahoo.com

[1] Separation Processes Research Laboratory, Department of Chemical and Petroleum Engineering, Afe Babalola University, Ado-Ekiti, Ekiti State, Nigeria

many chemical, biological, and physical treatment processes (Samiey et al. 2014; Xing et al. 2022). This is due to its high removal efficiency, low cost, simplicity of operation, low energy consumption, wide availability, and many more (Xu et al. 2014). Other methods proved to form large quantities of slug, generate secondary waste, and have exorbitant operational costs (Lakherwal 2014). High cost of commercial activated carbon has stimulated researchers to use agricultural by-products and wastes such as palm oil shells (Arami-Niyaa et al. 2012), sawdust (Yasmin and Zeki 2007), coconut shell (Yang et al. 2010), sugar cane bagasse (Karria et al. 2020), walnut shell (Popoola 2019), rice husk (Popoola 2020), and soya bean hulls (Nagh and Hanafiah 2008) as adsorbents for the treatment of heavy metal-polluted wastewater before discharge. This is due to their richness in lignin, cellulose, pectin, and numerous other compounds. Functional groups such as carbonyl, hydroxyl, carboxylic, amino, and alkoxy are present in these compounds which make them have a high affinity for metal ions present in wastewater and improve their adsorption capacities (Chu et al. 2020). Chemically modified adsorbents from agrowastes usually exhibit higher adsorption capacities than the unmodified adsorbents (Nagh and Hanafiah 2008). This is because pores of cellulose fibers in unmodified adsorbents are often occupied by many viscous compounds such as pectin and lignin (Abdel-Halim and Al-Deyab 2012).

Garcinia kola, also called African wonder nut, is an edible seed used medicinally in Africa as antiparasitic, anti-inflammatory, purgative, antiatherogenic, antidiabetic, antimicrobial, and immunomodulatory agent. It is also used in the treatment of bronchitis, liver disorders, diarrhea, hepatitis, throat infection, and so on (Moneim and Sulieman 2019). Its pharmaceutical and nutritional strengths are due to the presence of phytochemicals (alkaloids, tannins, flavonoids, saponins, and cyanogeinic glycosides) and nutrients (vitamins, proteins, minerals, and carbohydrates) (Adeyeye et al. 2007). *Garcinia kola*, which belongs to the family Guttiferae, is grown in coastal rainforests of Nigeria in the south-eastern and south-western parts. It is also found in some other African countries like Ghana, Cameroon, Senegal, Gabon, Benin, Congo, Gambia, Liberia, and Sierra Leone. In Nigeria, It is called "mijin-goro" in Hausa, "orogbo" in Yoruba, and "akiilu" in Igbo (Arekemase et al. 2012). High consumption of *Garcinia kola* has greatly influenced the volume of its hull generated on a daily basis which constitutes environmental pollution. The hull is highly rich in protein, fiber, and cellulose (Eleyinmi et al. 2006; Odebunmi et al. 2009) and also contains bioactive compounds such as flavonoids, alkaloids, tannins, saponins, and cyanogenic glycosides (Moneim and Sulieman 2019). The active compounds of *Garcinia kola* hull contain –OH and –COOH as major functional groups which have affinity to remove Cr(VI) from the solution via electrostatic and ionic bonding. The use of sodium hydroxide as the modification agent helps in breaking down the long cellulose chains of the hull particles. Nonetheless, the sodium hydroxide reacts with the active functional groups in the pre-hydrolyzed hull particles and influences the increase in pore openings available for the Cr(VI) sequestration (Homagai et al. 2010).

In previous studies, agrowaste materials such as oak sawdust (Argun et al. 2007), magnetic chitosan resins (Elwakeel 2010), banana peels (Ali and Saeed 2015), *Sterculia villosa* Roxb. shells (Patra et al. 2019), chickpea (Ozsin et al. 2019), and rice straw (Liu et al. 2020) were chemically modified and used as adsorbent for Cr(VI) removal from aqueous solution. Recently, chemically modified natural materials used as adsorbent for Cr(VI) sequestration from solution include bentonite (Castro-Castro et al. 2020), cellulose-based aerogel beads functionalized with amine (Li et al. 2022), and polypyrrole/natural pyrite composites (Zhang et al. 2022). In the study presented by Yusuff et al. (2022), biochar used as adsorbent for Cr(VI) removal from aqueous solution was prepared via modification of eucalyptus bark using $ZnCl_2$. The Freundlich and pseudo-second-order models best described the equilibrium data and adsorption kinetics of the process. In another recent study, a new biosorbent prepared via chemical modification of *Areca catechu* using H_2SO_4 for Cr(VI) sequestration was presented by Basnet et al. (2022). Experimental data were noticed to best be described by pseudo-second-order kinetic and the Langmuir isotherm models. Adsorption of Cr(VI) was suggested to be endothermic and spontaneous in nature. Polypyrrole nanotube and polypyrrole nanoparticle, prepared under various polymerization conditions of pyrrole monomers, had recently been used for Cr(VI) adsorption in aqueous solution (Choe et al. 2022a). Kinetics, isotherm equilibrium, and thermodynamics studies revealed experimental data to be well-fitted into pseudo-second-order kinetic and Langmuir isotherm models. In a related study, Choe et al. (2022b) applied a photocatalyst material prepared via traditional conductive polymer polypyrrole nanotube and metal-organic framework materials (NH_2-MIL-125) to reduce Cr(VI) concentration in solution. The result revealed 99.02% Cr(VI) reduction by 5% polymer polypyrrole nanotube@NH_2-MIL-125. Zhu et al. (2022) prepared novel interconnected hierarchical nickel-carbon hybrids which were assembled via porous nanosheets to reduce Cr(VI) in solution with formic acid. A recent study removed 97.62% of Cr(VI) from aqueous solution using a novel mesoporous Santa Barbara Amorphous-15 supported with Fe/Ni bimetallic composite (Xing et al. 2023).

In this study, chemically modified *Garcinia kola* hull particles (cMGK-HP) were *uniquely* applied as adsorbent for the sequestration of Cr(VI) from aqueous solution. The study of isotherm, kinetics, mechanics, and thermodynamics of the adsorption process is needed to effectively design

an industrial-based adsorption column as a component of waste treatment plant which removes Cr(VI) from industrial wastewater and aqueous streams in a large scale. This study adopts a batch-adsorption technique which is equivalent to a pilot-scale adsorption process to remove Cr(VI) from a simulated solution using an adsorbent prepared from *Garcinia kola* hull particles via chemical modification using sodium hydroxide. This can be integrated into a full-scale industrial level. The adsorbent can be placed in a designed packed adsorption column operated at required process conditions while allowing Cr(VI) wastewater to pass through on an industrial scale. Thus, this study predicts isotherm, kinetic, mechanistic, and thermodynamic parameters for Cr(VI) sequestration from solution with the aid of already existing mathematical models which were simulated using laboratory experimental data. Prior to this, the effect of pH, contact time, adsorbent dose, initial Cr(VI) concentration, and temperature on pollutant adsorption from solution was investigated. Unmodified and chemically modified adsorbents were characterized before and after Cr(VI) adsorption using BET, SEM, XRD, FTIR, TGA, and EDS. Adsorption mechanism was proposed, and adsorbent regeneration and reusability studies were executed.

Materials and methods

Chemicals and stock solution preparation

In this study, pure analytical grade chemicals were used without further alteration. A stock solution of 1000 mg/L of Cr(VI) was prepared via dissolving 2.8255 g of $K_2Cr_2O_7$ salt in 1000 mL of distilled water. Various concentrations (10, 20, 30, 40, 50, and 60 mg/L) of Cr(VI) needed for the experimental work were prepared by diluting the stock solution with distilled water. The solution pH was adjusted using either 0.1 M NaOH or 0.1 M HCl solutions.

Adsorbent preparation

Collected hulls of *Garcinia kola* from a local market were thoroughly washed with tap water and then rinsed with distilled water to remove unwanted impurities. Hulls were sun-dried for 7 days and oven-dried at 105°C for 48 h to remove retained water. The dried hulls were mechanically milled into fine particles, and an electric sieve shaker was used to obtain particle size of less than 150 µm. The hull particles (500 g) were alkali-hydrolyzed with 500 mL of 10% NaOH in a round bottom flask for 3 h at 120 rpm under reflux. The particles were cooled, filtered, thoroughly washed with distilled water till neutrality, and then dried in an oven for 24 h at 105°C. This breaks down the long cellulose chains into smaller monomers and also removes pectin and lignin present. The obtained filtrate was treated with phenolphthalein to know the degree of sample neutrality. During alkaline hydrolysis, a reaction between NaOH and acidic –OH/any free –COOH in the pre-hydrolyzed *Garcinia kola* hull particles (GK-HP) occurs. This forms the chemically modified *Garcinia kola* hull particles (cMGK-HP) used in this study and also develops suitable complexation sites for the removal of Cr(VI) from the solution. The untreated (raw) *Garcinia kola* hull particles (rGK-HP) was also kept in a tight nylon and placed in a desiccator for comparison purpose.

Instruments for samples characterization

Effect of chemical modification on textural characteristics of cMGK-HP was studied by the Brunauer-Emmett-Teller method with the aid of Quantachrome Autosorb instrument (Nova 11.03A, USA version) using physical nitrogen adsorption principle at 77 K. Sample structural morphology and elemental composition were determined using scanning electron microscope (SEM/EDX-JEOL-JSM 7600F) at ×5000, 15 kV. The phase composition of chemically modified GK-HP was studied using powder X-ray diffractometer (Rigaku D/Max-III, Tokyo, Japan) which employed Cu K α radiation (0.154 Å). Several functional groups present in rGK-HP and cMGK-HP were detected using FTIR spectrometer (Nicolet iS10 FT-IR Spectrometer) between wavelengths of 600–4000 cm^{-1} before and after Cr(VI) adsorption from solution. TGA analyzer (PerkinElmer; analysis condition: heating rate = 30°C min^{-1}, N_2 carrier flow rate = 20 mL min^{-1}, and temperature range = 30–800°C) was used to detect the thermal decomposition trend.

Batch adsorption step

Isotherm, kinetic, mechanistic, and thermodynamic studies of Cr(VI) sequestration from aqueous solution by rGK-HP and cMGK-HP were done. Batch adsorption process was executed at pH (2, 4, 6, 8, 10, and 12), contact time (20, 40, 60, 80, 100, and 120 min), adsorbent dose (2, 4, 6, 8, 10, and 12 g/L), Cr(VI) initial concentration (10, 20, 30, 40, 50, and 60 mg/L), and temperature (20, 30, 40, 50, and 60°C). The adsorbent, in specified quantity, was mixed with 50 mL of Cr(VI) salt solutions in a 250-mL flask for batch experiments. The flask was placed on a temperature-controlled heater (Stuart heat-stirrer SB162) operated at 160 rpm, specified temperature and time. The Whatman filter paper was used to separate the filtrate (stored in sample bottles) and residue (wrapped with aluminum foil and placed in a desiccator for laboratory analysis to avoid contamination). The concentrations of Cr(VI) in stored filtrates were determined using Atomic Adsorption Spectrophotometer (Buck scientific model 210 VGP). Percentage of Cr(VI) removed from

aqueous solution (X, %) and sorption capacity of GK-HP (q_e, mg/g) were determined using Eqs. (1) and (2), respectively.

$$X(\%) = \frac{(C_o - C_e)}{C_o} \times 100\% \quad (1)$$

$$q_e = (C_o - C_e) \times \frac{V}{W} \quad (2)$$

where C_o and C_e are the initial and final concentrations of Cr(VI) (mg/L) respectively, V is the solution volume (L), and W is the adsorbent weight (g).

Regeneration and reusability of GK-HP

Consecutive adsorption-desorption experiments were done to substantiate the reusability capacity of cMGK-HP for Cr(VI) sorption from aqueous solution. The first adsorption experiment was conducted by adding 0.5 g of Cr(VI) ions loaded cMGK-HP to 50 mL of 0.1 M HNO_3 solution in a flask (operated at 80°C and stirred for 2 h). After this, cMGK-HP was washed thoroughly with distilled water at 7.0 pH, dried for 6 h at 80°C, and reused consecutively for five times. Desorption efficiency was calculated using the method prescribed by Giri et al. (2011).

Results and discussions

Batch adsorption experiments

Effect of pH

Adsorption of chromium is greatly affected by aqueous solution pH. It has significant effects on Cr(VI) speciation and ionization degree as well as adsorbent surface charge (Labied et al. 2018; Popoola 2020). As the solution pH was increased from 2.0 to 12.0, Cr(VI) ion removed from the solution decreased significantly from 30.91 to 3.02% and 96.25 to 16.77% for rGK-HP and cMGK-HP, respectively (Fig. 1). Solution pH was adjusted using 0.1 M NaOH and 0.1 M HCl solutions. Though maximum Cr(VI) ion sequestration was obtained at optimum pH of 2 for both rGK-HP and cMGK-HP, alkaline hydrolysis of rGK-HP significantly enhanced the creation of more complexation sites for Cr(VI) removal. All further experiments were conducted at this optimum pH. Similar results were reported using chemically modified almond green hull waste material (Nasseh et al. 2017), walnut shell-Fe catalysts (Derdour et al. 2018), and *Areca catechu* (Basnet et al. 2022) with maximum hexavalent chromium removal of 99.96%, 98.89%, and 99.19%, respectively, at optimum pH of 2.

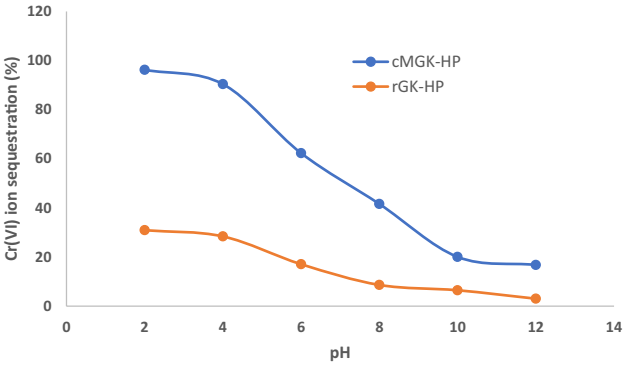

Fig. 1 Effect of pH on Cr(VI) ion sequestration from aqueous solution by rGK-HP and cMGK-HP. Temperature, 40°C; stirring rate, 120 rpm; solution volume, 50 mL; adsorbent dose, 5 g/L, contact time, 60 min; Cr(VI) initial concentration, 20 mg/L

Cr(VI) exists as $Cr_2O_7^{2-}$ and $HCrO_4^-$ in solution at the optimum pH for its adsorption. At acidic pH, the dominant form is $HCrO_4^-$ which is released as a result of dichromate ion $Cr_2O_7^{2-}$ hydrolysis. Highly protonated adsorbent surface favors Cr(VI) removal in this predominant anionic form which increases the amount removed from solution. As the pH deviates from acidic to basic, increase in the effluent concentration of $Cr_2O_7^{2-}$ becomes noticeable. At this point, active site dissociation occurs on the adsorbent surface and makes it to be negatively charged. This makes the complexation of negatively charged Cr(VI) anions difficult (due to repulsive forces), and thus, reduction in the percentage of Cr(VI) sequestration was observed.

Contact time effect

The percentage of Cr(VI) ion removal from solution increased from 26.71 to 50.55% and 78.38 to 98.91% when the contact time was increased from 20 to 120 min for rGK-HP and cMGK-HP, respectively (Fig. 2). Higher adsorption of Cr(VI) ion by cMGK-HP could be attributed to an increase in the number of active sites of the adsorbent as a result of the chemical modification of rGK-HP. However, optimum adsorption equilibrium time was reached by both adsorbents at 60 min. Before this time, bulk of adsorption was noticed due to higher forces of attraction between the active sites on adsorbents' surface and the Cr(VI) ions. No significant change was noticed in the equilibrium concentration when the reaction time was increased further from 60 to 120 min. Within this period, equilibrium was attained, and there was limitation in the number of adsorbents' active sites. At this point, the rate of sequestration is controlled by the Cr(VI) transportation rate from the exterior to the interior sites of rGK-HP and cMGK-HP. Similar findings were reported in previous studies (Ali et al. 2016; Nasseh et al. 2017; Basnet et al. 2022).

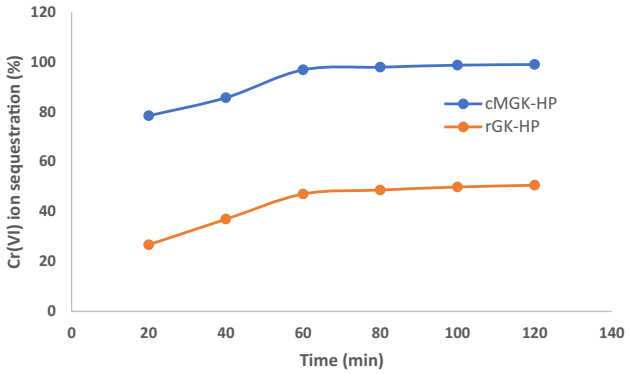

Fig. 2 Effect of contact time on Cr(VI) ion sequestration from aqueous solution by rGK-HP and cMGK-HP. Temperature, 40°C; stirring rate, 120 rpm; solution volume, 50 mL; adsorbent dose, 5 g/L; pH, 2; Cr(VI) initial concentration, 20 mg/L

Adsorbent dose effect

The study of adsorbent dose effect also revealed high significance of alkaline hydrolysis of the raw GK-HP on the Cr(VI) ion sequestration from aqueous solution. The percentage of Cr(VI) ion removed by cMGK-HP was higher than rGK-HP. As the adsorbent dose was increased from 2 to 12 g/L, the percentage of Cr(VI) ion removed from the solution increased from 19.33 to 45.18% and 84.81 to 96.10% for rGK-HP and cMGK-HP, respectively (Fig. 3). Increase in adsorbent dose increases the number of active sites on adsorbent surface. However, above adsorbent dose of 8 g/L, equilibrium was attained with no significant Cr(VI) removal. This resulted from the saturation of the available active sites. The result obtained was similar to those presented by Mandina et al. (2013) and Khan et al. (2017) where chemically modified orange peel and guar gum-nano zinc oxide were used for hexavalent chromium removal from aqueous solution, respectively.

Effect of Cr(VI) ion initial concentration

According to Fig. 4, the percentage of Cr(VI) ion removed from aqueous solution decreased from 28.99 to 12.48% and 91.91 to 49.03% using rGK-HP and cMGK-HP, respectively, at a constant dose of 8 g/L. The reduction in the percentage of Cr(VI) ion removed from aqueous solution could be linked to reduction in the number of active sites on the adsorbent surface as the initial concentration of Cr(VI) ion was increased. Constant percentage of Cr(VI) ion removal was attained after 50 mg/L and 40 mg/L of initial concentration of the pollutant for rGK-HP and cMGK-HP, respectively. At these points, the adsorbent surface is highly saturated, and further increase in the initial concentration of Cr(VI) ion has no significant effect on its percentage removal. The current results conform with the studies of Ali and Saeed (2015) where Cr(VI) was decontaminated from aqueous medium using untreated and chemically treated banana peel. Similarly, the study conducted by Nasseh et al. (2017) using almond green hull waste material as adsorbent revealed a decrease in the percentage of Cr(VI) removed from the aqueous as the initial concentration of Cr(VI) was increased.

Effect of temperature

As shown in Fig. 5, increasing the temperature from 20 to 60°C increases the percentage of Cr(VI) ion sequestration from 20.41 to 41.75% and 83.58 to 93.42% using rGK-HP and cMGK-HP, respectively. These results could be attributed to an increase in the convective movement of adsorbent particles due to temperature increase (Li et al. 2022).

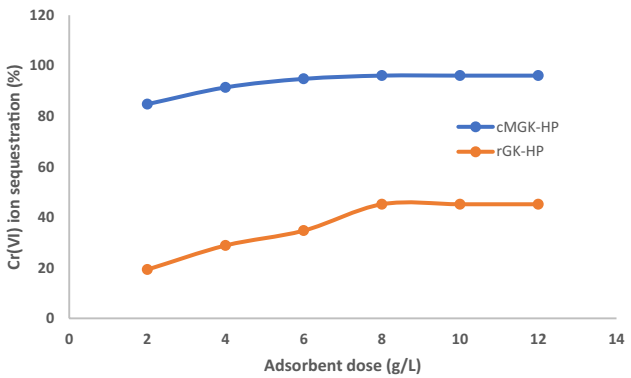

Fig. 3 Effect of adsorbent dose on Cr(VI) ion sequestration from aqueous solution by rGK-HP and cMGK-HP. Temperature, 40°C; stirring rate, 120 rpm; solution volume, 50 mL; contact time, 60 min; pH, 2; Cr(VI) initial concentration, 20 mg/L

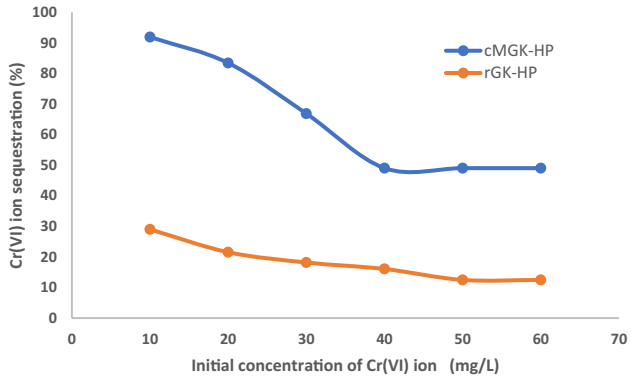

Fig. 4 Effect of initial concentration of Cr(VI) ion on its percentage removal from aqueous solution by rGK-HP and cMGK-HP. Temperature, 40°C; stirring rate, 120 rpm; solution volume, 50 mL; contact time, 60 min; pH, 2; adsorbent dose, 8 g/L

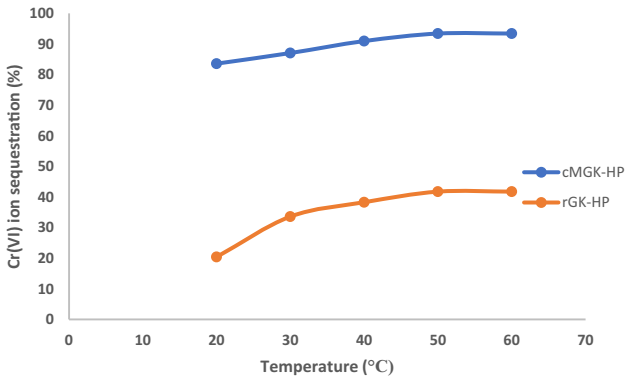

Fig. 5 Effect of temperature on Cr(VI) ion percentage removal from aqueous solution by rGK-HP and cMGK-HP. Cr(VI) initial concentration, 20 mg/L; stirring rate, 120 rpm; solution volume, 50 mL; contact time, 60 min; pH, 2; adsorbent dose, 8 g/L

Adsorption isotherm

In this study, linearized forms of two-parameter isotherm models were considered. These include the Freundlich (Freundlich 1906), the Langmuir (Langmuir 1916), and the Dubinin-Radushkevich (Dubinin and Radushkevich 1947), stated as Eqs. 3–5, respectively.

$$\log q_e = \log K_F + \frac{1}{n}\log C_e \tag{3}$$

$$\frac{C_e}{q_e} = \frac{1}{K_L q_{\max}} + \frac{C_e}{q_{\max}} \tag{4}$$

$$\mathrm{In}\left(q_e\right) = Inq_{D-R} - B_D\varepsilon^2 \tag{5}$$

where q_e is the adsorption capacity (mg/g), K_F is the Freundlich isotherm constant ($mg^{1-1/n}\,L^{1/n}\,g^{-1}$), n is the heterogeneity constant, C_e is the adsorbate equilibrium concentration (mg/L), K_L is the Langmuir constant (L mg^{-1}), q_{max} is the Langmuir maximum adsorption capacity (mg g^{-1}), $q_{D\text{-}R}$ is the D-R adsorbent maximum monolayer adsorption capacity (mg g^{-1}), B_D is the D-R isotherm constant of adsorption energy ($mol^2\,kJ^{-2}$), and ε is the Polanyi potential related to equilibrium concentration (Eq. 6).

$$\varepsilon = RTIn\left(1 + \frac{1}{C_e}\right) \tag{6}$$

where R is the universal gas constant (8.314 J mol^{-1} K^{-1}) and T is the absolute temperature (°K).

The dimensionless separation factor (R_L) is calculated using Eq. 7. It determines whether an adsorption process is favorable ($0 < R_L < 1$), linear ($R_L = 1$), unfavorable ($R_L > 1$), or irreversible ($R_L = 0$).

$$R_L = \frac{1}{1 + K_L C_o} \tag{7}$$

The adsorption nature of D-R isotherm was analyzed using adsorption mean energy (E, kJ/mol) given as Eq. 8.

$$E = \frac{1}{\sqrt{\left(-2B_D\right)}} \tag{8}$$

The results obtained for the plots of Freundlich ($log\ q_e$ versus $log\ C_e$) (Fig. 6), Langmuir (C_e/q_e versus C_e) (Fig. 7), and D-R (lnq_e versus $ln(1 + 1/C_e)^2$) (Fig. 8) are summarized in Table 1. The R^2 values obtained, using rGK-HP and cMGK-HP as adsorbents for Cr(VI) removal from aqueous solution, for Langmuir (0.9715 and 0.9984) were greater than and closer to unity than those of Freundlich (0.8048 and 0.8780) and Dubinin-Radushkevich (0.9679 and 0.9801), respectively. This suggests that the Langmuir isotherm is appropriate to represent the sequestration of Cr(VI) from aqueous solution by cMGK-HP. Also, this is a strong indication that monolayer adsorption of Cr(VI) occurred on the surface of adsorbents with homogenous adsorption affinity

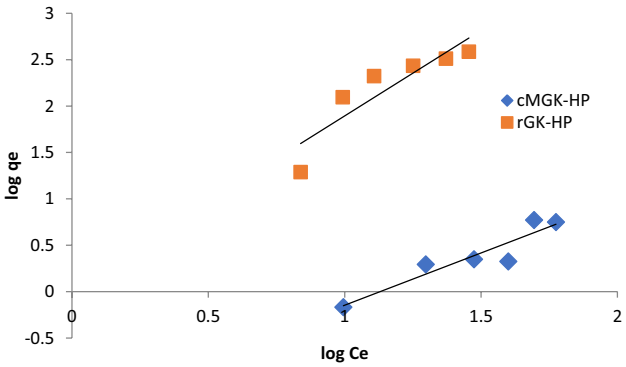

Fig. 6 Freundlich plot of $log\ q_e$ versus $log\ C_e$

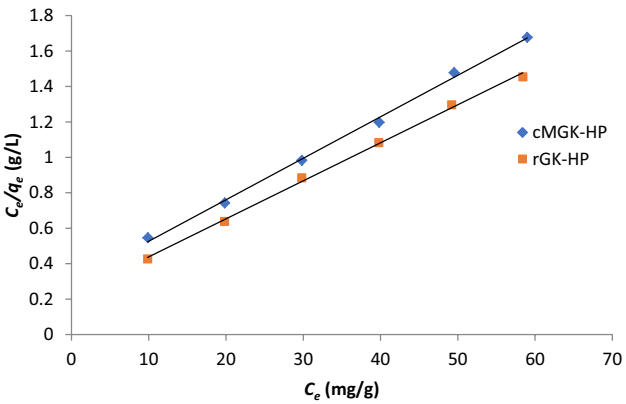

Fig. 7 Langmuir plot of C_e/q_e versus C_e

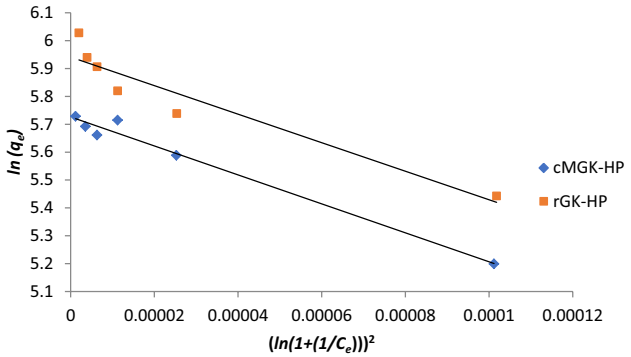

Fig. 8 Dubinin-Radushkevich plot of lnq_e versus $ln(1 + 1/C_e)^2$

and energy distribution characteristics (Langmuir 1918). The maximum adsorption capacity obtained for Cr(VI) removal using rGK-HP (60.24 mg g^{-1}) and cMGK-HP (217.39 mg g^{-1}) under the Langmuir isotherm suggested that the adsorbents are effective for the sequestration of Cr(VI) at pH, temperature, and time of 2, 40°C, and 60 min, respectively. In the previous studies, equilibrium data presented using kernel shell (Parlayici and Pehlivan 2019) and banana peel (Ali et al. 2016) also conformed to Langmuir isotherm with maximum adsorption capacity of 10.42 mg g^{-1} and 4.15 mg g^{-1}, respectively. Table 2 summarizes the adsorption capacities of adsorbents used in previous and present studies for Cr(VI) removal from solution and their efficiencies.

Nonetheless, the Freundlich isotherm revealed values of n for rGK-HP (1.8622) and cMGK-HP (2.7248) to be greater than 1 suggesting a favorable adsorption of Cr(VI) on the adsorbents. This is also supported by the values of R_L obtained for the respective adsorbents (0.6362 and 0.8633) being less than 1. The values of E obtained from the D-R isotherm model revealed the amount of E in Cr(VI) adsorption by rGK-HP and cMGK-HP to be 26.49 and 26.84 kJ/mol, respectively. This suggests that physical adsorption took part in the process under the examined conditions, and thus, sequestration of Cr(VI) by rGL-HP and cMGK-HP occurred by the physisorption mechanism.

Adsorption kinetics

Adsorption kinetics help in predicting the removal rate of a pollutant from solution, and it is a function of the adsorbent physicochemical characteristics. It also significantly reveals the best fit model in designing an adsorption system. Equations 9 and 10 represent the respective linearized forms of pseudo-first-order and pseudo-second-order kinetic models used in this study.

$$In\left(q_e - q_t\right) = Inq_e - k_1 t \tag{9}$$

$$\frac{t}{q_t} = \frac{1}{k_2 q_e^2} + \frac{t}{q_e} \tag{10}$$

where q_e is the equilibrium experimental adsorption capacity (mg g^{-1}), q_t is the adsorption capacity at time t (mg g^{-1}), k_1 = pseudo-first-order rate constant (min^{-1}), and k_2 is the pseudo-second-order rate constant (g mg^{-1} min^{-1}).

Table 1 Result summary of two-parameter isotherm models for Cr(VI) removal

Isotherm models	Results	
	rGK-HP	cMGK-HP
Freundlich		
Fitted model	$\log q_e = 0.0494 + 0.537 \log C_e$	$\log q_e = -1.2733 + 0.367 \log C_e$
K_F	1.1205	0.0533
n	1.8622	2.7248
R^2	0.8048	0.8780
Langmuir		
Fitted model	$\frac{C_e}{q_e} = 0.2904 + 0.0166 C_e$	$\frac{C_e}{q_e} = 0.2693 + 0.0046 C_e$
K_L	0.0572	0.0158
R_L	0.6362	0.8633
q_{max}	60.24	217.39
R^2	0.9915	0.9984
Dubinin-Radushkevich		
Fitted model	$\ln(q_e) = 6.415 + 4825.9\varepsilon^2$	$\ln(q_e) = 6.9381 + 4406.2\varepsilon^2$
$q_{D\text{-}R}$	610.94	1030.81
B_D	7.13×10^{-4}	6.94×10^{-4}
E	26.4881	26.8352
R^2	0.9679	0.9801

Table 2 Adsorption capacities and removal efficiencies of some previously used adsorbents for Cr(VI) removal

Adsorbent	Adsorption capacity (mg/g)	Removal efficiency (%)	Reference
Walnut shell-Fe	29.67	–	Derdour et al. (2018)
Rice husk	10.18	85.5–98.5	Mitra et al. (2019)
Peanut shell	22.94	87.8	Das et al. (2019)
Almond shell	24.25	90.2	
Walnut shell	24.52	92.2	
$MnFe_2O_4$-/polyaniline nanocomposite	175.44	99.01	Das et al. (2020)
Aspergillus carbonarius-sodium alginate	–	92.43	Lakshmi et al. (2020)
Rice husk-H_3PO_4	23.91	99.88	Vunain et al. (2021)
Potato peel-H_3PO_4	20.76	99.52	
Arundo donax stem	76.92	> 90	Bhattarai et al. (2022)
Chemically modified dormant *Aspergillus niger* spores	177	91	Ren et al. 2022
Al embedded groundnut shell	13.458	94.2	Vaddi et al. (2022)
$ZnCl_2$-Eucalyptus bark biochar	36.18	94.47	Yusuff et al. (2022)
$CaFe_2O_4/ZrO_2$ -MNC	178.57	95	Bhowmik et al. (2022)
Pomegranate peel-H_2SO_4	82.99	98.03	Rai et al. (2023)
Santa Barbara Amorphous-15/Fe/Ni	180.99	97.62	Xing et al. (2023)
Eichhornia crassipes	–	98.4	Fito et al. (2023)
rGK-HP	60.24	30.91	This study
cMGK-HP	217.39	96.25	This study

Equation 11 represents the intra-particle diffusion model (Weber and Morris 1963) used to examine the mechanism of Cr(VI) diffusion from bulk solution onto the adsorbent using kinetic data from experimental work.

$$q_t = K_{id}t^{0.5} + C \tag{11}$$

where K_{id} is the intraparticle diffusion rate constant (mg g^{-1} $min^{-0.5}$) and C is the boundary layer diffusion effect constant (mg g^{-1}).

A plot of $ln(q_t\text{-}q_e)$ versus t (Fig. 9) for the pseudo-first-order kinetic model gives a straight line used in determining k_1 and R^2. Similarly, a plot of t/q_t versus t (Fig. 10) for the pseudo-second-order kinetic model gives a straight line used in determining k_2 and R^2. The slope and intercept of a non-linear plot of q_t versus $t^{0.5}$ (Fig. 11) give the value of K_{id} and C, respectively. The value of the correlation coefficient, R^2, from the plots, determines the best fit between the kinetic models. Table 3 gives information about the kinetic parameters and fitted model. The result revealed that the process of Cr(VI) sequestration from aqueous solution by rGK-HP and cMGK-HP follows and conforms to the pseudo-second-order kinetic model ($R^2 > 0.99$). Similar studies on Cr(VI) removal from aqueous solution presented similar results (Parlayici and Pehlivan 2019; Basnet et al. 2022). The plot of q_t versus $t^{0.5}$ as shown in Fig. 11 did not pass through the origin, and also, the values of C (Table 3) deviated marginally from zero, suggesting intra-particle diffusion occurred during

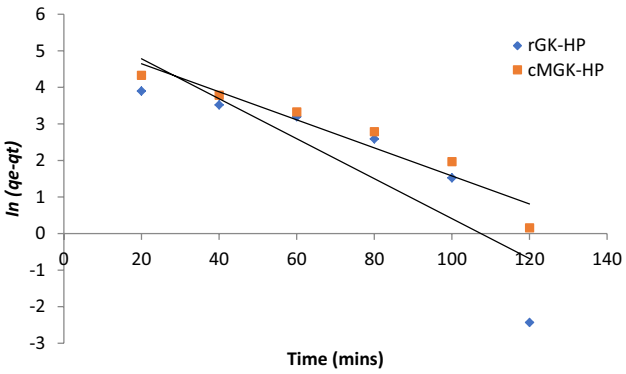

Fig. 9 Pseudo-first-order kinetic plots of Cr(VI) sequestration by rGK-HP and cMGK-HP

Cr(VI) removal alongside other adsorption mechanisms (Zhu et al. 2018). This was earlier justified in the result presented when examining the contact time effect on Cr(VI) sequestration from aqueous solution by these adsorbents (see the "Contact time effect" section).

Adsorption thermodynamics

Equations 12 and 13 were used to estimate the change in the standard Gibbs free energy (ΔG^o), standard enthalpy

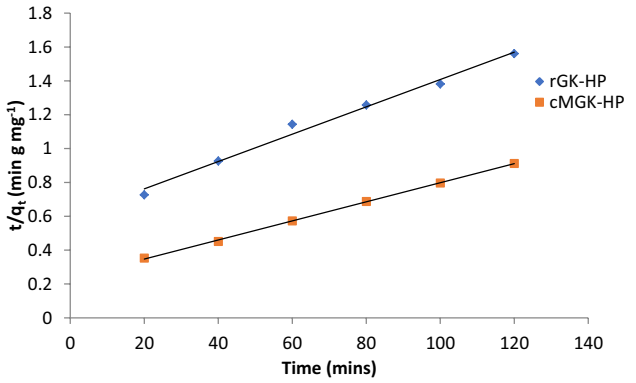

Fig. 10 Pseudo-second-order kinetic plots of Cr(VI) sequestration by rGK-HP and cMGK-HP

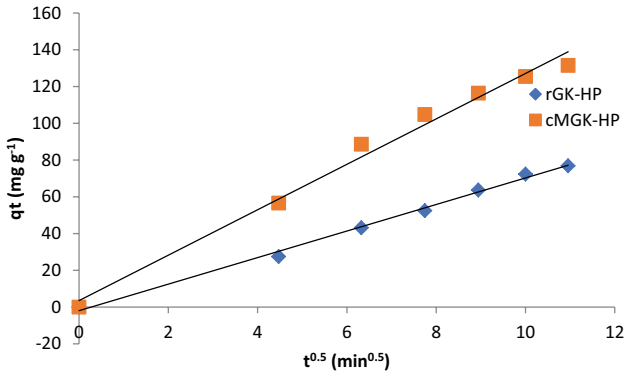

Fig. 11 Intra-particle diffusion plots of Cr(VI) sequestration by rGK-HP and cMGK-HP

(ΔH^o), and standard entropy (ΔS^o) to determine the thermodynamics nature of Cr(VI) sequestration from solution by rGK-HP and cMGK-HP.

$$\Delta G^o = \Delta H^o - T\Delta S^o \tag{12}$$

$$InK_L = \frac{\Delta S^o}{R} - \frac{\Delta H^o}{RT} \tag{13}$$

where R is the 8.314 $Jmol^{-1}K^{-1}$ (universal gas constant), K_L is the Langmuir constant due to binding sites affinity and adsorption energy and T (°K) is the absolute temperature. Values of ΔH^o and ΔS^o are, respectively, the slope and intercept from a plot of lnK_L versus $1/T$ (Fig. 12). These values are substituted into Eq. 12 at different temperatures to obtain ΔG^o presented in Table 4. The values of ΔH^o and ΔG^o were negative which strongly suggest adsorption of Cr(VI) was spontaneous, feasible, and exothermic in nature (Bhatt et al. 2015). The value of ΔG^o increased with an increase in temperature which suggests strong adsorption feasibility at higher temperatures. Also, the range of ΔG^o values suggests adsorption to occur by physisorption (Labied et al. 2018). Nonetheless, the positive values of ΔS^o for both rGK-HP and cMGK-HP indicate a high degree of disorderliness at the solid-liquid interface during Cr(VI) adsorption onto the adsorbents (Popoola 2020). Similar result was presented by Ali et al. (2016), but at higher temperatures, ΔG^o values decreased with increasing temperature suggesting a decline in Cr(VI) adsorption feasibility. In the result presented by Basnet et al. (2022), adsorption of Cr(VI) onto chemically modified *Areca catechu* was endothermic in nature.

Characterization

Brunauer-Emmett-Teller analysis

Table 5 compares the BET results of rGK-HP and cMGK-HP used in this study with adsorbents used for Cr(VI) removal from aqueous solution in previous studies. From the results presented, cMGK-HP proved to be a better adsorbent for Cr(VI) removal with improved surface area, total pore volume, and average pore diameter of 221.75 m^2/g, 0.267 cm^3/g, and 58.44 Å, respectively, than previous adsorbents except for chemically modified oil palm frond and coconut shell used by Zainol et al. (2017) and Amenyah Kove et al. (2021) with surface area and total pore volume of 700 m^2/g and 0.32 cm^3/g and 787.88 m^2/g and 0.415 cm^3/g, respectively. However, the values obtained are closer to those presented by Yusuff et al. (2022) in which $ZnCl_2$-modified eucalyptus bark biochar was used as adsorbent for Cr(VI) removal from aqueous solution. Nonetheless, chemical modification of raw *Garcinia kola* hull particles via alkaline hydrolysis with NaOH greatly improved its textural properties when compared with untreated *Garcinia kola* hull particles having surface area, total pore volume, and average pore diameter of 52.93 m^2/g, 0.092 cm^3/g, and 18.11 Å, respectively.

The BET N_2 adsorption-desorption curve for rGK-HP and cMGK-HP, presented as Fig. 13a, b, respectively,

Table 3 Kinetic parameters of Cr(VI) sequestration from aqueous solution by rGK-HP and cMGK-HP

	$q_{e(exp)}$	Pseudo-first-order			Pseudo-second-order			Intra-particle diffusion		
		$k_1 \times 10^{-2}$	$q_{e,(cal)}$	R^2	$k_2 \times 10^{-3}$	$q_{e,(cal)}$	R^2	K_{id}	C	R^2
rGK-HP	9.926	3.32	5.427	0.9023	2.24	9.745	0.9901	4.81	1.13	0.9810
cMGK-HP	13.951	4.04	8.473	0.8941	1.96	13.454	0.9989	5.77	1.48	0.9473

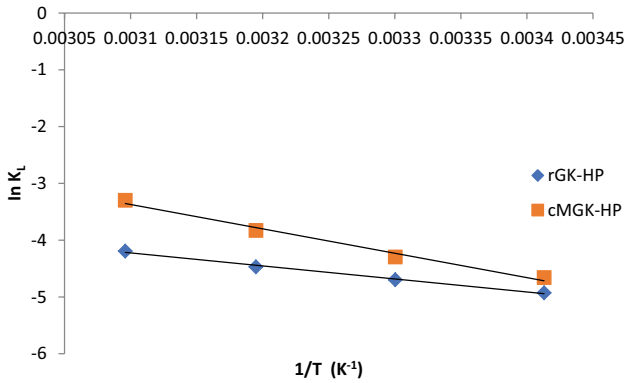

Fig. 12 Plot of ln K_L versus 1/T (K^{-1}) for Cr(VI) sequestration by rGK-HP and cMGK-HP at 20–50°C

revealed the BET isotherms to be type IV (Zhang et al. 2020). At low relative pressure, the isotherm is convex, suggesting strong affinity of the adsorbent for the adsorbate. As the relative pressure increases, gradual transition of multilayer adsorption to capillary condensation occurs. Under this condition, the increase in adsorption isotherm within a particular pressure range makes the curve to be steeper and increases the adsorption rate. As the relative pressure approaches unity, the curve becomes relatively flat suggesting the occurrence of adsorption saturation. However, the volume of adsorbed N_2 by cMGK-HP was higher than rGK-HP, indicating that the former has more pores than the latter due to the chemical modification by NaOH. Figure 14a reveals cMGK-HP to possess a higher surface area than rGK-HP. Figure 14b represents the pore size distribution and cMGK-HP possesses broad pore size distribution in the range of 0.2–63 nm as compared to rGK-HP which possesses 0.1–18 nm. This result suggests the presence of macropores and mesopores in cMGK-HP (Wang et al. 2014).

Scanning electron microscopy analysis

The SEM micrographs of rGK-HP and cMGK-HP before and after Cr(VI) sequestration from aqueous solution are presented in Fig. 15. The image depicts the presence of few micropores on rGK-HP surface which is unevenly distributed and rough in nature (Fig. 15a). The pores were filled up and blocked with Cr(VI) after sequestration, which makes the surface to be relatively smooth (Fig. 15b). Figure 15c depicts the surface morphology of cMGK-HP showing formation of more micropores due to chemical modification of the cellulosic compounds present in raw GK-HP. After Cr(VI) sequestration, the number of pores drastically reduced (Fig. 15d) as a result of blockage by the Cr(VI), which makes the surface not to be too smooth. The SEM images of rGK-HP and cMGK-HP before Cr(VI) sequestration were subjected to ImageJ, and average pore diameters of 17.39 Å and 60.16 Å were, respectively, obtained. The values were close to those

Table 4 Thermodynamic parameters for Cr(VI) sequestration from solution by rGK-HP and cMGK-HP

	ΔS^o (J/mol K)	ΔH^o (kJ/mol)	R^2	ΔG^o (kJ/mol)			
				20°C	30°C	40°C	50°C
rGK-HP	+24.12	−19.11	0.9945	−26.18	−26.42	−26.66	−26.90
cMGK-HP	+34.91	−27.66	0.9985	−37.89	−38.24	−38.59	−38.94

Table 5 Comparison of BET results of different adsorbents prepared from agrowastes for Cr(VI) removal

Agrowastes	Total pore volume (cm^3/g)	Surface area (m^2/g)	Average pore diameter (Å)	Reference
Tamarind wood	0.0567	101.51	22.35	Sahu et al. (2009)
Peanut shell	–	72.48	4.50	Ilyas et al. (2012)
Citrus cinensis	0.000246	0.8311	23.699	Mandina et al. (2013)
Oil palm frond	0.32	700.00	5.85	Zainol et al. (2017)
Raw walnut shell-rice husk	0.0073	38.08	2.77	Popoola (2019)
Calcinated walnut shell-rice husk	0.0932	94.54	3.31	Popoola (2019)
Magnetized walnut shell-rice husk	0.0811	126.72	4.18	Popoola (2019)
Coconut shell	0.4150	787.88	–	Amenyah Kove et al. (2021)
Eucalyptus bark biochar	0.04	48.4	11.6	Yusuff et al. (2022)
$ZnCl_2$-Eucalyptus bark biochar	0.21	217.3	49.9	Yusuff et al. (2022)
rGK-HP	0.092	52.93	18.11	This study
cMGK-HP	0.267	221.75	58.44	This study

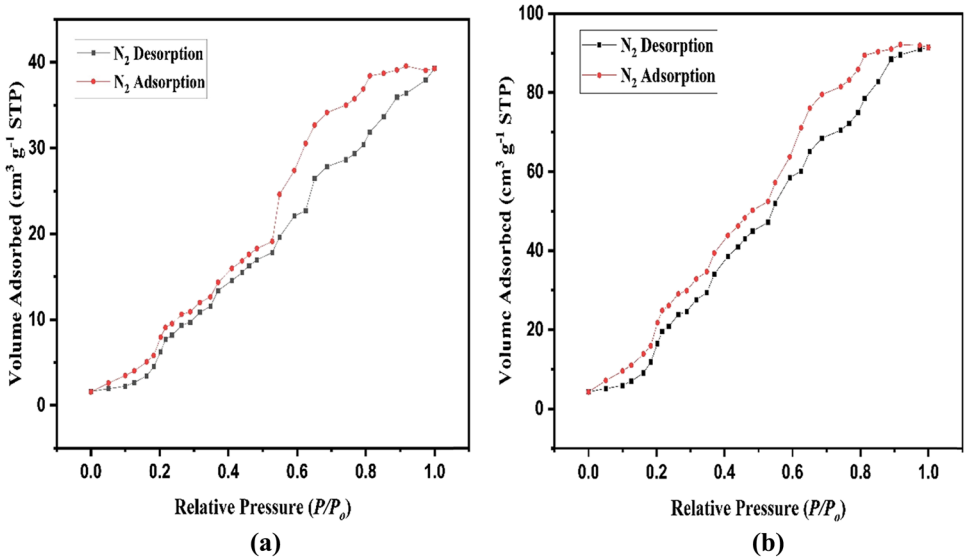

Fig. 13 BET N_2 adsorption-desorption curve for **a** rGK-HP and **b** cMGK-HP

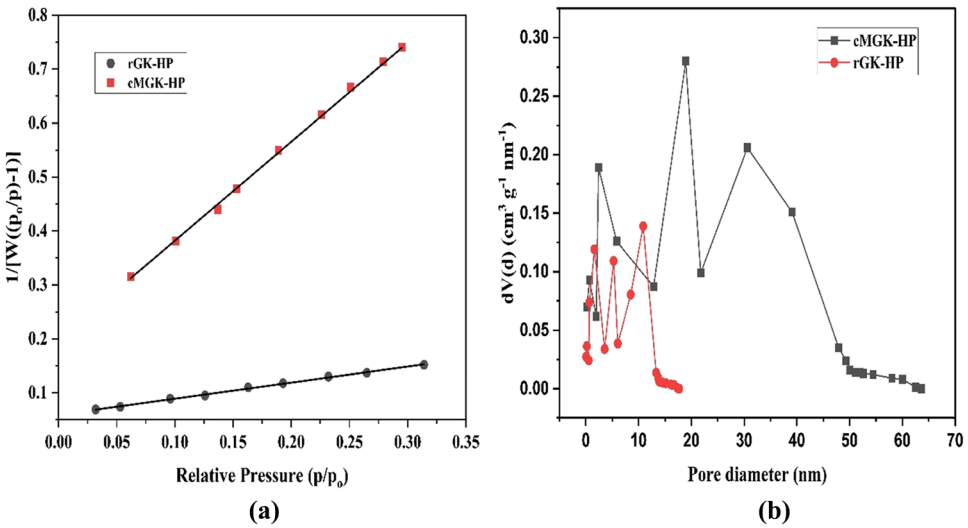

Fig. 14 BET **a** surface area and **b** pore size distribution for rGK-HP and cMGK-HP

obtained from the BET analysis. The results presented by Ali et al. (2016) were similar to this in which comparison was done between raw and chemically modified banana peels used as efficient low-cost adsorbent for Cr(VI) removal from aqueous medium.

Powder X-ray diffractometer analyses

The XRD patterns of rGK-HP and cMGK-HP at 2θ value between 0 and 70° are shown in Fig. 16. In both, peaks of quartz (2θ (27°, 50°, and 68°)), calcite (2θ (30°, 47°, and 49°)), and chlorite (2θ (5°, 13°, and 60°)) were predominant. However, peak transformation of berlinite (2θ (26° and 68°)) and sepiolite (2θ (8°, 20°, and 37°)) in rGK-HP (Fig. 16a) to gypsum (2θ (30° and 50°)) and sodalite (2θ (15° and 25°)) in cMGK-HP (Fig. 16b) occurred due to the chemical modification via NaOH hydrolysis.

Fourier transform infrared analyses

The FTIR spectra of as-prepared rGK-HP (Fig. 17a), cMGK-HP (Fig. 17b), and cMGK-HP after Cr(VI) removal (Fig. 17c) are presented. Peaks formed at 3295.0 cm^{-1}, 2885.0 cm^{-1}, 1599.0 cm^{-1}, 1420.1 cm^{-1}, 1252.4 cm^{-1}, 1028.7 cm^{-1}, and 872.2 cm^{-1} for rGK-HP (Fig. 17a) correspond to O-H stretching vibration due to hydrogen bonding in cellulose and protein (Pal et al. 2021); asymmetric stretching vibration of C-H in methyl group (Jia-Shun et al. 2014); stretching vibrations of –C=O (Popoola 2020); bending of –COOH in cellulose (Hero et al. 2012); stretching vibration of C-O in phenols, alcohols, or ether groups

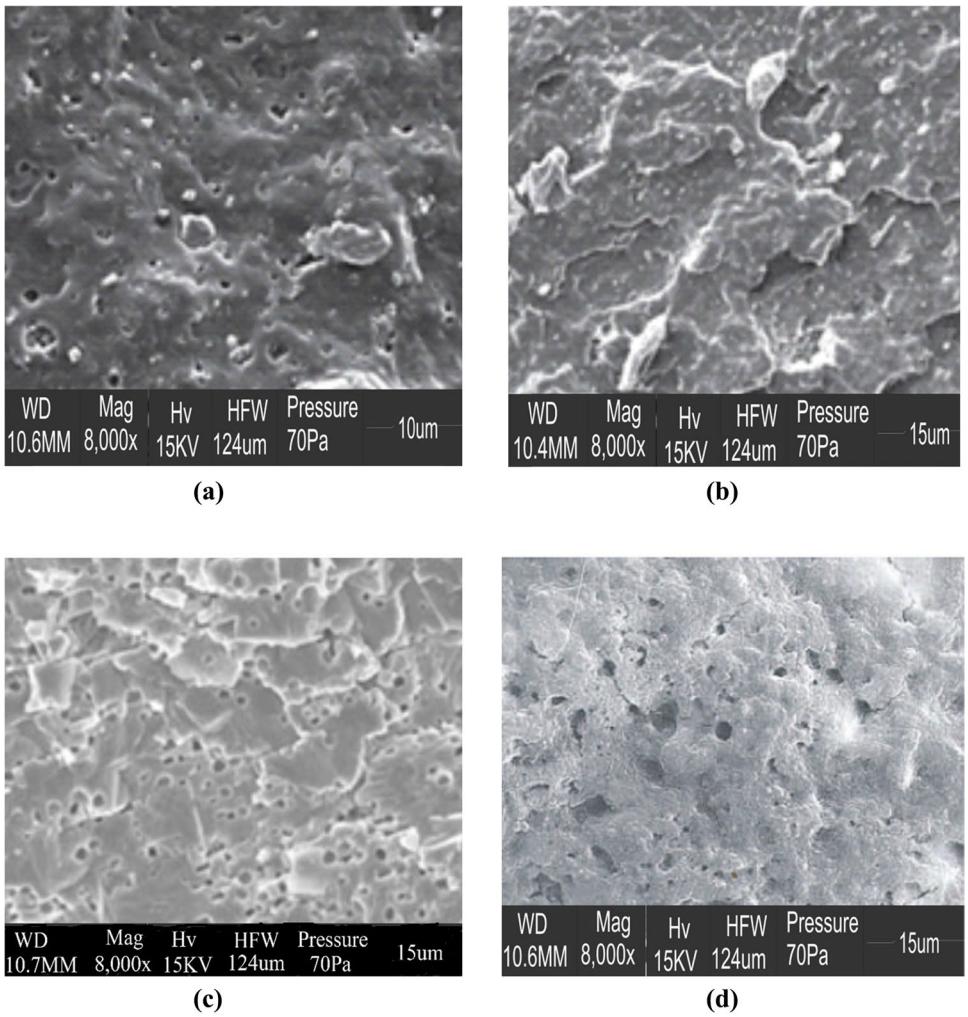

Fig. 15 SEM micrograph of rGK-HP **a** before and **b** after Cr(VI) sequestration and cMGK-HP **c** before and **d** after Cr(VI) sequestration at Cr(VI) initial concentration, 20 mg/L; stirring rate, 120 rpm; solution volume, 50 mL; contact time, 60 min; pH, 2; adsorbent dose, 8 g/L

(Jia-Shun et al. 2014); and deformation of C-H in cellulose (Asmaa and Muthanna 2016), respectively. However, the peak attributed to C-H asymmetric stretching vibration disappeared while that of C-O stretching vibration became weaker due to alkaline hydrolysis of *Garcinia kola* hull particles using NaOH (Fig. 17b). New sharp peaks were formed at 3332.2 cm^{-1} (strong -OH stretching vibration); 1636.3 cm^{-1} (strong C=O stretching); 1375.4 cm^{-1} (strong C-N stretching); 1155.5 cm^{-1} and 1032.5 cm^{-1} (strong C-O stretching), and 872.2 cm^{-1} (C-H out-of-plane deformation). Figure 17c strongly reveals the adsorption of Cr(VI) onto the micropores of cMGK-HP because shift in the peaks to 3118.1 cm^{-1}, 1630.6 cm^{-1}, and 1017.6 cm^{-1} was noticed. The new peak formed at 3652.8 cm^{-1} could be attributed to -NH_2 stretching of protein in cMGK-HP (Ghadir et al. 2015) as a result of Cr(VI) adsorption.

Thermogravimetric analyses

The TGA analyses of rGK-HP and cMGK-HP followed a similar trend (Fig. 18) but exhibited different weight loss characteristics due to the chemical modification. Loss in weight of 6.8% (rGK-HP) and 6.1% (cMGK-HP) was observed at 49.3°C due to evaporation of water. The second stage involves the decomposition of protein and occurred at 267.9°C (Zhou and Basile 2017). At this point, rGK-HP and cMGK-HP lost 37.4% and 29.2% of their weight. Weight loss of 56.4% (rGK-HP) and 37.7% (cMGK-HP) was noticed at the third stage. This was observed at 369.6°C due to the decomposition of the cellulosic material in the adsorbents (Su-Hwa et al. 2014; Wang et al. 2021). A relatively constant weight loss was observed for both adsorbents at the final stage. Finally, rGK-HP and cMGK-HP were able to retain 30.17% and 44.1% of their respective weight at 700°C. The hydrolysis of cMGK-HP using NaOH made it to have better thermal stability

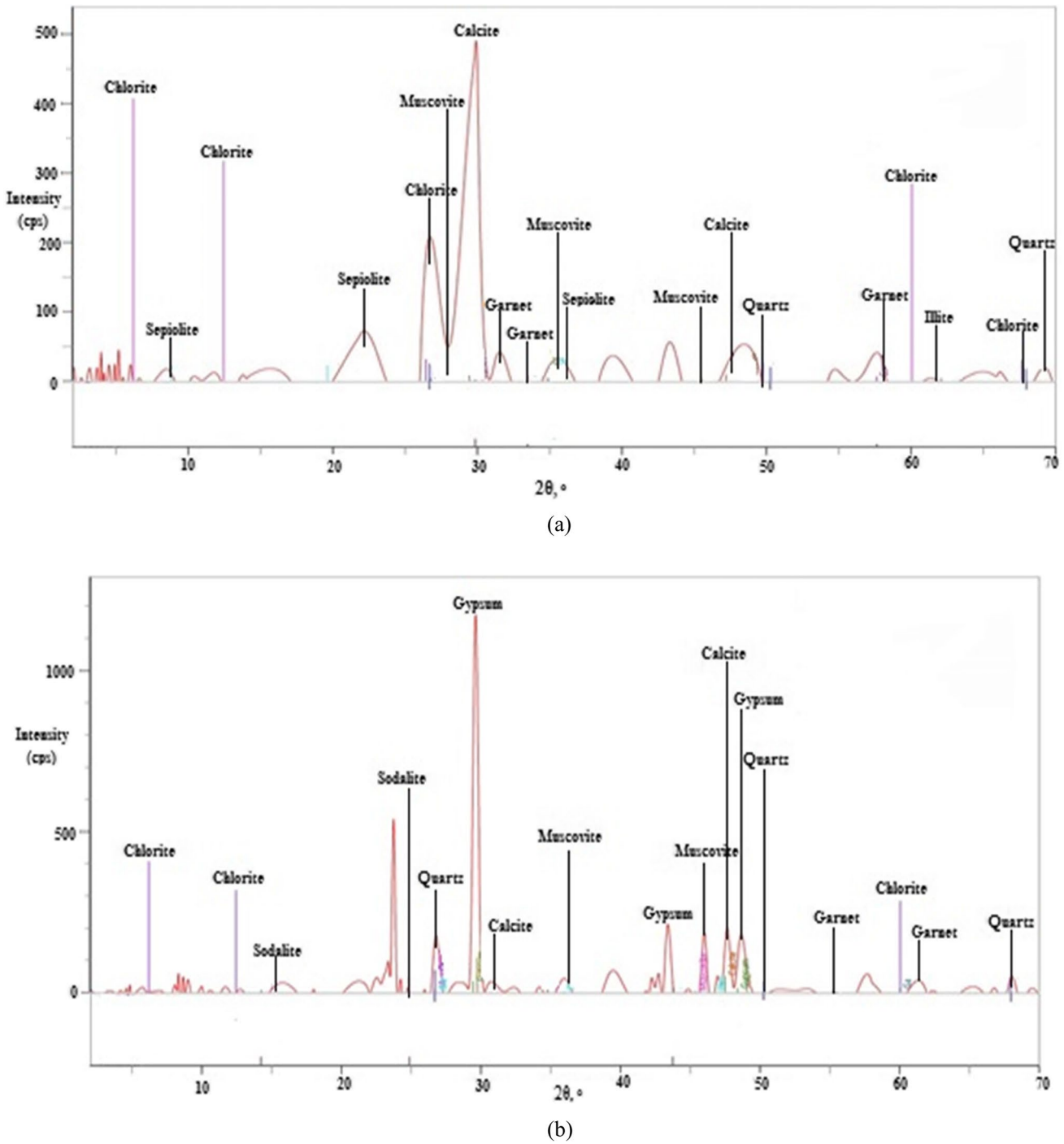

Fig. 16 Powder-XRD spectrum of **a** rGK-HP and **b** cMGK-HP

than rGK-HP. Similar trend was observed in the result of Derdour et al. (2018), where both raw and iron-modified walnut shells were used as adsorbents for hexavalent chromium removal from wastewater.

Energy dispersive spectroscopy analyses

The results of EDS analyses for rGK-HP and cMGK-HP before and after Cr(VI) removal from solution are presented

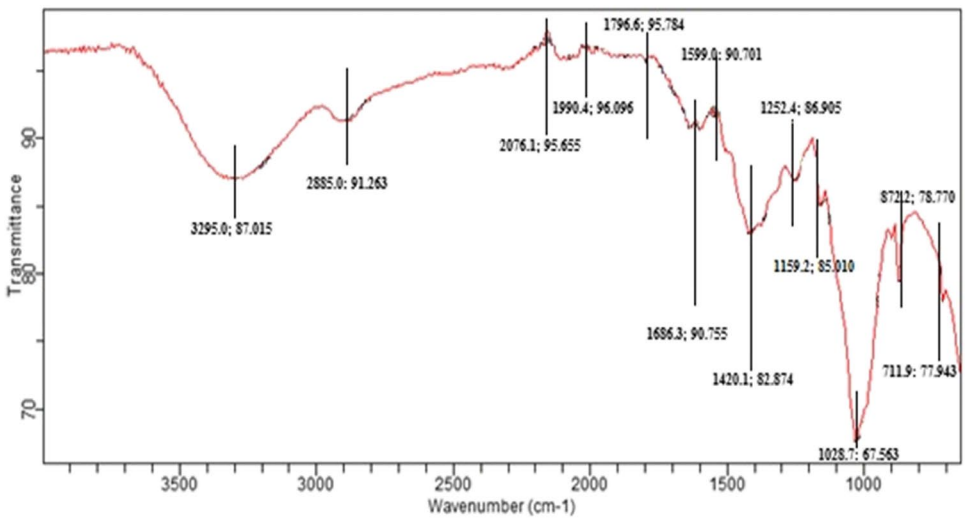

(a)

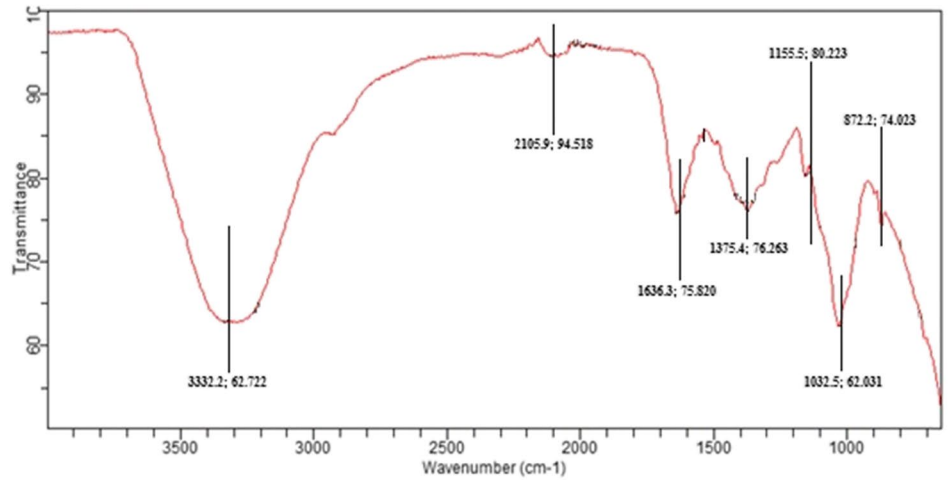

(b)

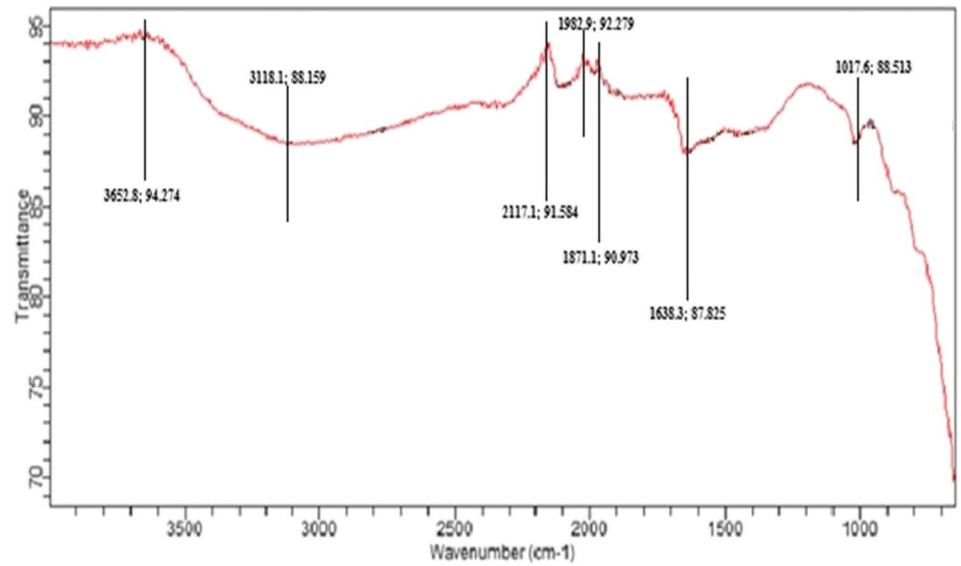

(c)

Fig. 17 FTIR spectrum of prepared **a** rGK-HP, **b** cMGK-HP, and **c** cMGK-HP after Cr(VI) sequestration

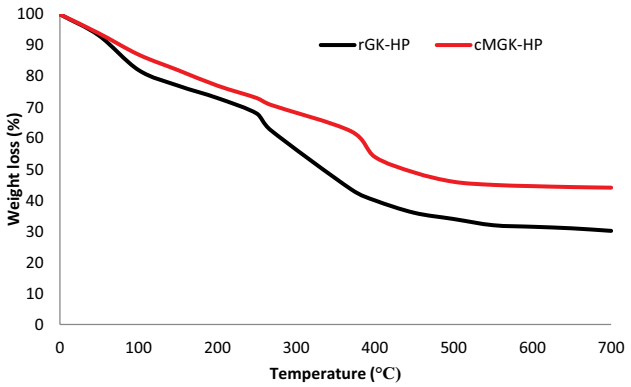

Fig. 18 TGA of rGK-HP and cMGK-HP

Table 6 EDS of rGK-HP and cMGK-HP before and after Cr(VI) sequestration

Element	Before sequestration (wt%)		After sequestration (wt%)	
	rGK-HP	cMGK-HP	rGK-HP	cMGK-HP
Ca	12.16	13.67	12.32	12.77
Si	22.59	21.76	23.11	19.52
Al	2.46	1.48	3.52	3.14
C	12.77	4.55	10.35	3.11
S	2.18	1.05	3.62	1.35
K	6.99	6.24	6.44	6.52
Na	2.36	11.74	2.16	8.48
Mg	9.23	4.8	9.2	3.87
H	12.51	14.56	11.04	13.63
O	16.75	20.15	14.39	18.34
Cr	ND	ND	3.85	9.27

in Table 6. The elemental compositions of adsorbents are presented in weight %. The presence of Ca, Si, Al, C, S, K, Na, Mg, H, and O were noticed with different weight % in both adsorbents before Cr(VI) sequestration. However, the weight % of Na, H, and O was higher in cMGK-HP due to the reaction between NaOH and acidic –OH/any free –COOH in pre-hydrolyzed *Garcinia kola* hull particles during hydrolysis using NaOH. Generally, variations in the elemental compositions of rGK-HP and cMGK-HP could be linked to the chemical modifications of the protein, fiber, and cellulose present in raw *Garcinia kola* hull particles (Idris-Hermann et al. 2018). Nonetheless, the presence of Cr was noticed in both adsorbents after the removal due to Cr(VI) adsorption from the solution by the adsorbent particles. However, cMGK-HP recorded higher Cr composition (9.27 wt%) than rGK-HP (3.93 wt%) due to an increase in surface area, creation of more pores, and presence of active functional groups, as evident in earlier presented BET, SEM, and FTIR results due to the NaOH hydrolysis. This enables cMGK-HP to have better affinity for Cr(VI) removal from aqueous solution.

Adsorption mechanisms

At a low pH, the surfaces of rGK-HP and CMGK-HP are positively charged and, thus, become protonated. The amount of Cr(VI) adsorbed increased due to attraction between H^+ ions and oxy-anions (CrO_4^{2-} and $Cr_2O_7^{2-}$) formed in solution according to Eqs. 14 and 16. Also, the adsorbent matrix (see SEM results presented in Fig. 15 a, c) enhanced the adsorption by interacting with Cr(VI) ion via complexion and electrostatic interaction (Gorzin et al. 2018). Electrostatic attraction also comes into play between Cr(VI) ions and oxygen-oriented functional groups (OH^-, –COOH, and C=O) on the adsorbent surface (see FTIR results presented in Fig. 17 a, b). This also increases the volume of Cr(VI) removed from the solution.

At high pH values, adsorbents' surface becomes negatively charged. Thus, OH^- ions in solution and chromium compound oxy-anions compete together, thereby reducing the amount of Cr(VI) removed from solution. Similar studies that used bio-waste adsorbents (Parlayici and Pehlivan 2019), Pongamia pinnata seeds (Brungesh et al. 2015), corn stalk (Guo et al. 2020), and $ZnCl_2$-modified eucalyptus bark (Yusuff et al. 2022) to remove Cr(VI) ion from solution also presented similar adsorption mechanisms.

$$\text{At low pH}: HCr_2O_7 \rightarrow H^+ + HCr_2O_7^{2-} \quad (14)$$

$$HCr_2O_4 \rightarrow H^+ + HCrO_{4^-} \quad (15)$$

$$\text{At high pH}: Cr_2O_7^{2-} \rightarrow OH^- \rightarrow HCrO_{4^-} + CrO_4^{2-} \quad (16)$$

$$HCrO_{4^-} + OH^- \rightarrow CrO_4^{2-} + H_2O \quad (17)$$

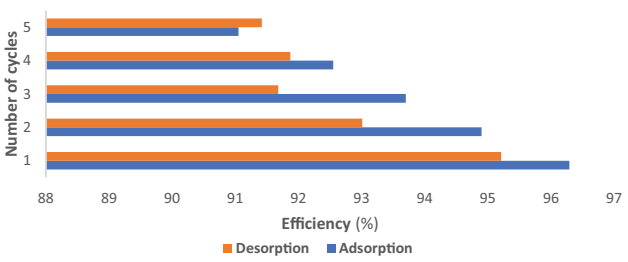

Fig. 19 Cr(VI) Adsorption-desorption efficiency after five cycles using cMGK-HP

Regeneration and reusability of GK-HP

As shown in Fig. 19, the percentage of Cr(VI) removed from the solution decreased with increasing adsorption-desorption cycle number. After the fifth regeneration of cMGK-HP, the percentage of Cr(VI) removed from the solution decreased from 96.29 to 91.05%. This could be attributed to the loss of some active sites on the adsorbent surface during dissolution. Also, the result revealed high potential of cMGK-HP to be used repeatedly for Cr(VI) sequestration from the solution because the percentage removal was even greater than 90% after the fifth cycle. The cMGK-HP is robust and has high stability (as also revealed by TGA, see Fig. 18) for the sequestration of Cr(VI) from the solution.

Conclusions

Comparative analyses between using rGK-HP and cMGK-HP for Cr(VI) sequestration from solution have been executed in this study. Chemically modified GK-HP proved more effective for Cr(VI) sequestration than rGK-HP. It possesses excellent thermal stability, textural, and reusability attributes. It can remove 96.25% of Cr(VI) from the solution at a pH of 2, a temperature of 40°C, an adsorbent dose of 5 g/L, a contact time of 60 min, and Cr(VI) initial concentration of 20 mg/L. Sequestration of Cr(VI) from aqueous solution by cMGK-HP conformed to the Langmuir isotherm and pseudo-second-order kinetic model. Adsorption nature was feasible, physisorption, spontaneous, and exothermic with high degree of disorderliness. SEM, BET, FTIR, XRD, and EDS revealed change in morphological structure, textural property, spectral peak, phase composition, and chemical composition of rGK-HP and cMGK-HP before and after Cr(VI) sequestration from solution. In conclusion, the adsorption capacity of cMGK-HP is better than many other adsorbents generated from agro-wastes used in previous studies for Cr(VI) removal.

Author contribution This declaration is not applicable.

Funding The author acknowledges the financial support by the Afe Babalola University, Ado-Ekiti, Nigeria, towards the publication of this research article.

Data availability The data used to support the findings of this study are included within the article.

Declarations

Ethical approval This declaration is not applicable.

Consent to participate This declaration is not applicable.

Consent for publication This declaration is not applicable.

Competing interests The author declares no competing interests.

References

Abdel-Halim ES, Al-Deyab SS (2012) Chemically modified cellulosic adsorbent for divalent cations removal from aqueous solutions. Carbohydr Polym 87(2):1863–1868

Adeyeye EI, Asaolu SS, Aluko AO (2007) Amino acid composition of two masticatory nuts (Cola acuminata and Garcinia kola) and a snack nut (Anacardium occidentale). Int J Food Sci Nutr 58(4):241–249

Ali A, Saeed K (2015) Decontamination of Cr(VI) and Mn(II) from aqueous media by untreated and chemically treated banana peel: a comparative study. Desalination Water Treat 35(11):3586–3591

Ali A, Saeed K, Mabood F (2016) Removal of chromium (VI) from aqueous medium using chemically modified banana peels as efficient low-cost adsorbent. Alex Eng J 55:2933–2942

Amenyah Kove EP, Buah WK, Dankwa OK, Mends EA (2021) Attenuation of heavy metals from waste oil-based drilling mud using locally produced activated carbon. Ghana Mining Journal 21(2):55–61

Arami-Niyaa A, Daud WMAW, Mjalli FS, Abnisa F, Shafeeyan MS (2012) Production of microporous palm shell based activated carbon for methane adsorption: modeling and optimization using response surface methodology. Chem Eng Res Des 90:776–784

Arekemase MO, Aliyu MB, Kayode RM, Ajiboye AE, Ajijolakewu AK (2012) Antimicrobial effects of Garcinia Kola (bitter kola) on some selected pathogens from University of Ilorin Teaching Hospital Ilorin, Nigeria. J Asian Sci Res 2(4):159–169

Argun ME, Dursun S, Ozdemir C, Karatas M (2007) Heavy metal adsorption by modified oak sawdust: thermodynamics and kinetics. J Hazard Mater 141:77–85

Asmaa FA, Muthanna JA (2016) Mesoporous activated carbon from date stones (Phoenix dactylifera L.) by one-step microwave assisted K_2CO_3 pyrolysis. J Water Process Eng 9:201–207

Basnet P, Ojha PK, Gyawali D, Ghimire KN, Paudyal H (2022) Thermochemical study of Cr(VI) sequestration onto chemically modified Areca catechu and its recovery by desorptive precipitation method. Heliyon 8:e10305

Bhatt R, Sreedhar B, Padamaja P (2015) Adsorption of chromium from aqueous solutions using cross-linked chitosan diethylenetriamine-penta acetic acid. Int J Biol Macromol 74:458–466

Bhattarai KP, Pant BD, Rai R, Aryal RL, Paudyal H, Gautam SK, Ghimire KN, Pokhrel MR, Poudel BR (2022) Efficient sequestration of Cr(VI) from aqueous solution using biosorbent derived from Arundo donax Stem. J Chem 2022:9926391, 12. https://doi.org/10.1155/2022/9926391

Bhowmik M, Debnath A, Saha B (2022) Scale-up design and treatment cost analysis for abatement of hexavalent chromium and metanil yellow dye from aqueous solution using mixed phase CaFe2O4 and ZrO2 nanocomposite. Int J Environ Res 16(5):80

Brungesh KV, Nagabhushana BM, Raveendra RS, Krishna HR, Prashantha PA, Nagabhushana H (2015) Adsorption of Cr(VI) from aqueous solution onto a mesoporous carbonaceous material prepared from naturally occurring Pongamia pinnata seeds. J Environ Anal Toxicol 5(6):1

Castro-Castro JD, Macías-Quiroga IF, Giraldo-Gómez GI, Sanabria-González NR (2020) Adsorption of Cr(VI) in aqueous solution using a surfactant-modified bentonite. Scientific World Journal 3628163:9. https://doi.org/10.1155/2020/3628163

Choe JN, Ji JM, Yu JH, Jang KJ, Yun J, Choe SJ, Rim YI, Jo CN (2022a) Adsorption of Cr(VI) in aqueous solution by polypyrrole nanotube and polypyrrole nanoparticle; kinetics, isotherm

equilibrium, and thermodynamics. Inorg Chem Commun 145:109981
Choe JN, Yang X, Yu JH, Jang KJ, Kim MB, An KC (2022b) Visible-light responsive PPynt@NH_2-MIL-125 nanocomposite for efficient reduction of Cr(VI). Colloids Surf A Physicochem Eng Asp 636:128147
Chu Y, Zhu S, Xia M, Wang F, Lei W (2020) Methionine-montmorillonite composite – a novel material for efficient adsorption of lead ions. Adv Powder Technol 31:708–717
Das A, Banerjee M, Bar N, Das SK (2019) Adsorptive removal of Cr(VI) from aqueous solution: kinetic, isotherm, thermodynamics, toxicity, scale-up design, and GA modeling. SN Appl Sci 1:776
Das P, Nisa S, Debnath A, Saha B (2020) Enhanced adsorptive removal of toxic anionic dye by novel magnetic polymeric nanocomposite: optimization of process parameters. J Dispers Sci Technol. https://doi.org/10.1080/01932691.2020.1845958
Derdour K, Bouchelta C, Naser-Eddine AK, Medjram MS (2018) Removal of Cr(VI) from aqueous solutions by using activated carbon supported iron catalysts as efficient adsorbents. World J Eng 15(1):3–13
Dubinin MM, Radushkevich LV (1947) Equation of the characteristic curve of activated charcoal proceedings of the Academy of Sciences. Physical Chemistry Section USSR 55:331–333
Eleyinmi AF, Bressler DC, Amoo IA, Sporns P, Oshodi AA (2006) Chemical composition of bitter cola (Garcinia kola) seed and hulls. Pol J Food Nutr Sci 56(4):395–400
Elwakeel KZ (2010) Removal of Cr(VI) from alkaline aqueous solutions using chemically modified magnetic chitosan resins. Desalination 250(1):105–112
Fernandez PM, Vinarta SC, Bernal AR, Cruz EL, Figueroa LIC (2018) Bioremediation strategies for chromium removal: current research, scale-up approach and future perspectives. Chemosphere 208:139–148
Fito J, Tibebu S, Nkambule TTI (2023) Optimization of Cr (VI) removal from aqueous solution with activated carbon derived from Eichhornia crassipes under response surface methodology. BMC Chemistry 17:4. https://doi.org/10.1186/s13065-023-00913-6
Freundlich HMF (1906) Over the adsorption in solution. J Phys Chem 57:385–471
Ghadir N, Hossein A, Mohamad E (2015) Batch adsorption of cephalexin antibiotic from aqueous solution by walnut shell-based activated carbon. J Taiwan Inst Chem Eng:1–9
Giri SK, Das NN, Pradhan GC (2011) Synthesis and characterization of magnetite nanoparticles using waste iron ore tailings for adsorptive removal of dyes from aqueous solution. Colloids Surf A Physicochem Eng Asp 389:43–49
Gorzin F, Rasht B, Abadi MM (2018) Adsorption of Cr(VI) from aqueous solution by adsorbent prepared from paper mill sludge: kinetics and thermodynamics studies. Ads Sci Techn 36(1–2):149–169
Guo X, Liu A, Lu J, Niu X, Jiang M, Ma Y, Liu X, Li M (2020) Adsorption mechanism of hexavalent chromium on biochar: kinetic, thermodynamic and characterization studies. ACS Omega 5(42):27323–27331
Hamilton EM, Young SD, Bailey EH, Watts MJ (2018) Chromium speciation in foodstuffs: a review. Food Chem 250:105–112
Hero M, Ruiz B, Andrade M, Mester AS, Parra JB, Carvalho AP, Ania CO (2012) Dual role of copper on the reactivity of activated carbons from coal and lignocellulosic precursors. Microporous Mesoporous Mater 154:68–73
Homagai PL, Ghimire KN, Inoue K (2010) Adsorption behavior of heavy metals onto chemically modified sugarcane bagasse. Bioresour Technol. 101(6):2067–2069
Idris-Hermann KT, Raoul TTD, Giscard D, Gabche AS (2018) Preparation and characterization of activated carbons from bitter kola (Garcinia kola) nut shells by chemical activation method using H_3PO_4; KOH and $ZnCl_2$. Chem Sci Int J 23(4):1–15
Ilyas M, Saeed M, Ahmad A (2012) Removal of Cr(VI) from aqueous solutions using peanut shell as adsorbent. J Chem Soc Pak 34(5):1197–1203
Jia-Shun C, Jun-Xiong L, Fang F, Ming-Ting Z, Zhi-Rong H (2014) A new absorbent by modifying walnut shell for the removal of anionic dye: kinetic and thermodynamic studies. Bioresour Technol 163:199–205
Karria RR, Sahu JN, Meikap BC (2020) Improving efficacy of Cr (VI) adsorption process on sustainable adsorbent derived from waste biomass (sugarcane bagasse) with help of ant colony optimization. Ind Crop Prod 143:111927
Khan TA, Nazir M, Ali I, Kumar A (2017) Removal of chromium (VI) from aqueous solution using guar gum–nano zinc oxide biocomposite adsorbent. Arab J Chem 10:2388–2398
Labied R, Benturki O, Hamitouche AYE, Donnot A (2018) Adsorption of hexavalent chromium by activated carbon obtained from a waste lignocellulosic material (Ziziphus jujuba cores): Kinetic, equilibrium and thermodynamic study. Adsorp Sci Technol 36(3–4):1066–1099
Lakherwal D (2014) Adsorption of heavy metals: a review. Int J Environ Res Develop 4(1):41–48
Lakshmi S, Suvedha K, Sruthi R, Lavanya J, Varjani S, Nakkeeran E (2020) Hexavalent chromium sequestration from electronic waste by biomass of Aspergillus carbonarius. Bioengineered 11(1):708–717
Langmuir I (1916) The constitution and fundamental properties of solids and liquids. Part I. Solids J Am Chem Soc 38:2221–2295
Langmuir I (1918) The adsorption of gases on plane surfaces of glass, mica and platinum. J Am Chem Soc 40:1361–1401
Li M, He J, Tang Y, Sun J, Fu H, Wan Y, Qu X, Xu Z, Zheng S (2019) Liquid phase catalytic hydrogenation reduction of Cr(VI) using highly stable and active Pd/CNT catalysts coated by N-doped carbon. Chemosphere 217:742–753
Li M, Tang C, Fu S, Tam KC, Zong Y (2022) Cellulose-based aerogel beads for efficient adsorption-reduction-sequestration of Cr(VI). Int J Biol Macromol 216:860–870
Liu Q, Li Y, Chen H, Lu J, Yu G, Moslang M, Zhou Y (2020) Superior adsorption capacity of functionalized straw adsorbent for dyes and heavy-metal ions. J Hazard Mater 382:121040
Mandina S, Chigondo F, Shumba M, Nyamunda BC, Sebata E (2013) Removal of chromium (VI) from aqueous solution using chemically modified orange (citrus cinensis) peel. IOSR J Appl Chem 6(2):66–75
Mitra T, Bar N, Das SK (2019) Rice husk: green adsorbent for Pb(II) and Cr(VI) removal from aqueous solution—column study and GA–NN modeling. SN Appl Sci 1:486
Moneim A, Sulieman E (2019) Garcinia kola (Bitter Kola): chemical composition. In: Mariod A (ed) Wild Fruits: Composition, Nutritional Value and Products. Springer, Cham. https://doi.org/10.1007/978-3-030-31885-7_23
Nagh WS, Hanafiah MAKM (2008) nRemoval of heavy metal ions from wastewater by chemically modified plant wastes as adsorbents: a review. Bioresour Technol 99(10):3935–3948
Nasseh N, Taghavi L, Barikbin B, Harifi-Mood AR (2017) The removal of Cr(VI) from aqueous solution by almond green hull waste material: kinetic and equilibrium studies. J Water Reuse Desalin 7(4):447–459
Odebunmi EO, Oluwaniyi OO, Awolola GV, Adediji OD (2009) Proximate and nutritional composition of kola nut (Cola nitida), bitter cola (Garcinia kola) and alligator pepper (Afromomum melegueta). Afr J Biotechnol 8(2):308–310
Ogata F, Ueta E, Kawasaki N (2018) Characteristics of a novel adsorbent Fe–Mg-type hydrotalcite and its adsorption capability

of As(III) and Cr(VI) from aqueous solution. J Ind Eng Chem 59:56–63
Ozsin G, Kılıç M, Apaydın E, Pütün AE (2019) Chemically activated carbon production from agricultural waste of chickpea and its application for heavy metal adsorption: equilibrium, kinetic and thermodynamic studies. Appl Water Sci 9:56
Pal OB, Singh A, Jha JM, Srivastava N, Hashem A, Alakeel MA, Abdallah EF, Gupta VK (2021) Low-cost biochar adsorbents prepared from date and delonix regia seeds for heavy metal sorption. Bioresour Technol 339:125606
Parlayici S, Pehlivan E (2019) Comparative study of Cr(VI) removal by bio-waste adsorbents: equilibrium, kinetics and thermodynamic. J Anal Sci Technol 10(15):1–8
Patra C, Medisetti RMN, Pakshirajan K, Narayanasamy S (2019) Assessment of raw, acid-modified and chelated biomass for sequestration of hexavalent chromium from aqueous solution using Sterculia villosa Roxb. shells. Environ Sci Pollut Res 26:23625–23637
Popoola LT (2019) Nano-magnetic walnut shell-rice husk for Cd(II) sorption: design and optimization using artificial intelligence and design expert. Heliyon 5:e02381
Popoola LT (2020) Tetracycline and sulfamethoxazole adsorption onto nanomagnetic walnut shell-rice husk: isotherm, kinetic, mechanistic and thermodynamic studies. Int J Environ Anal Chem 100(9):1021–1043
Qiu J, Zhang XF, Zhang X, Feng Y, Li Y, Yang L, Lu H, Yao J (2018) Constructing $Cd_{0.5}Zn_{0.5}S$@ZIF-8 nanocomposites through self-assembly strategy to enhance Cr(VI) photocatalytic reduction. J Hazard Mater 349:234–241
Rai R, Aryal RL, Paudyal H, Gautam SK, Ghimire KN, Pokhrel MJ, Poudel BR (2023) Acid-treated pomegranate peel; an efficient biosorbent for the excision of hexavalent chromium from wastewater. Heliyon 9:e15698
Ren B, Jin Y, Zhao L, Cui C, Song X (2022) Enhanced Cr(VI) adsorption using chemically modified dormant Aspergillus niger spores: process and mechanisms. J Environ Chem Eng 10:106955
Sahu JN, Acharya J, Meikap BC (2009) Response surface modeling and optimization of chromium(VI) removal from aqueous solution using tamarind wood activated carbon in batch process. J Hazard Mater 172(2-3):818–825
Samiey B, Cheng CH, Wu J (2014) Organic–inorganic hybrid polymers as adsorbents for removal of heavy metal ions from solutions: a review. Materials 7(2):673–726
Song H, Liu W, Meng F, Yang Q, Guo N (2021) Efficient sequestration of hexavalent chromium by graphene-based nanoscale zero-valent iron composite coupled with ultrasonic pretreatment. Int J Environ Res Public Health 18:5921
Su-Hwa J, Seung-Jin O, Gyung-Goo C, Joo-Sik K (2014) Production and characterization of microporous activated carbons and metallurgical bio-coke from waste shell biomass. J Anal Appl Pyrolysis 109:123–131
Vaddi DR, Gurugubelli TR, Koutavarapu R, Lee DY, Shim J (2022) Bio-stimulated adsorption of Cr(VI) from aqueous solution by groundnut shell activated carbon@Al embedded material. Catalysts 12:290. https://doi.org/10.3390/catal12030290
Vunain E, Njewa JB, Biswick TT, Ipadeola AK (2021) Adsorption of chromium ions from tannery effluents onto activated carbon prepared from rice husk and potato peel by H_3PO_4 activation. Applied Water Science 11:150
Wang J, Minami E, Asmadi M, Kawamoto H (2021) Thermal degradation of hemicellulose and cellulose in ball-milled cedar and beech wood. J Wood Sci 67:32
Wang L, Schütz C, Salazar-Alvarez G, Titirici MM (2014) Carbon aerogels from bacterial nanocellulose as anodes for lithium ion batteries. RSC Adv 4:17549–17554
Weber WJ, Morris JC (1963) Kinetics of adsorption on carbon from solutions. J Sanit Eng Div Am Soc Civil Eng 89:31–60
Xing X, Alharbi NS, Ren X, Chen C (2022) A comprehensive review on emerging natural and tailored materials for chromium-contaminated water treatment and environmental remediation. J Environ Chem Eng 10(2):107325
Xing X, Ren X, Alharbi NS, Chen C (2023) Efficient adsorption and reduction of Cr(VI) from aqueous solution by Santa Barbara Amorphous-15 (SBA-15) supported Fe/Ni bimetallic nanoparticles. J Colloid Interface Sci 629:744–754
Xu CH, Zhu LJ, Wang XH, Lin S, Chen YM (2014) Fast and highly efficient removal of chromate from aqueous solution using nanoscale zero-valent Iron/Activated Carbon (NZVI/AC). Water Air Soil Pollut 225:1845
Yang K, Peng J, Srinivasakannan C, Zhang L, Xia H, Duan X (2010) Preparation of high surface area activated carbon from coconut shells using microwave heating. Bioresour Technol 101:6163–6169
Yao Y, Mi N, He C, Zhang Y, Yin L, Li J, Wang W, Yang S, He H, Li S, Ni L (2020) A novel colloid composited with polyacrylate and nano ferrous sulfide and its efficiency and mechanism of removal of Cr(VI) from Water. J Hazard Mater 399:123082
Yasmin B, Zeki T (2007) Removal of heavy metals from aqueous solution by sawdust adsorption. J Environ Sci 19:160–166
Yulizar Y, Kadja M, Yudiana A (2016) Fe(II)-MSA functionalized Au nanoparticle on natural zeolites as effective reducing agent for Cr(VI) ions. AIP Conf Proc 1729(1):020043
Yusuff AS, Lala MA, Thompson-Yusuff KA, Babatunde EO (2022) $ZnCl_2$-modified eucalyptus bark biochar as adsorbent: preparation, characterization and its application in adsorption of Cr(VI) from aqueous solutions. S. Afr J Chem Eng 42:138–145
Zainol MM, Asmadi M, Amin NAS (2017) Preparation and characterization of impregnated magnetic particles on oil palm frond activated carbon for metal ions removal. Sains Malaysiana 46(5):773–782
Zhang F, Xi L, Zhao M, Du Y, Ma L, Chen S, Ye H, Du D, Zhang TC (2022) Efficient removal of Cr(VI) from aqueous solutions by polypyrrole/natural pyrite composites. J Mol Liq 365:120041
Zhang M, Wang Y, Huang H, Shang F, Song X (2020) sol-gel-supercritical synthesis and properties of nitrocellulose/glycidylazide polymer/pentaerythritol tetranitrate nanocomposites. Int J Energ Mater Chem Propuls 19(2):135–147
Zhou R, Basile F (2017) Plasmonic thermal decomposition/digestion of proteins: a rapid on-surface protein digestion technique for mass spectrometry imaging. Anal Chem 89(17):8704–8712
Zhu H, Chen T, Liu J, Li D (2018) Adsorption of tetracycline antibiotics from an aqueous solution onto graphene oxide/calcium alginate composite fibers. RSC Adv 8:2616–2621
Zhu K, Chen L, Alharbi NS, Chen C (2022) Interconnected hierarchical nickel-carbon hybrids assembled by porous nanosheets for Cr(VI) reduction with formic acid. J Colloid Interface Sci 606(Part 1):213–222